Optics Communications 372 (2016) 166–171

Contents lists available at ScienceDirect

Optics Communications

journal homepage: www.elsevier.com/locate/optcom

Analysis of electromagnetic focusing properties of multi-annular nanostructured metasurfaces

Shuming Yang [a,b], Tong Wang [a,b], Tao Liu [a,b,*], Zhuangde Jiang [a,b]

[a] State Key Laboratory for Manufacturing System Engineering, Xi'an Jiaotong University, Xi'an 710049, China
[b] Collaborative Innovation Center of High-End Manufacturing Equipment, Xi'an Jiaotong University, Xi'an 710049, China

ARTICLE INFO

Article history:
Received 1 February 2016
Received in revised form
31 March 2016
Accepted 8 April 2016
Available online 16 April 2016

Keywords:
Metasurface
FDTD
Diffraction
Nanostructure
Polarization

ABSTRACT

To explore the electromagnetic focusing properties of multi-annular nanostructured metasurfaces, the material property, dispersion property, and error-tolerance property have been studied through a combination of the vectorial angular spectrum theory and the three-dimensional finite-difference time-domain (FDTD) method. An obvious focal shift has been observed and the thickness for the Ag, Al, and Au films is suggested to be within the range of 50–100 nm for the illumination wavelength of 640 nm. The light dispersion effect of the metasurface is remarkable and the focal length decreases with the increase of the wavelength; however, the on-axis intensity distributions retain a similar, shifted shape when the wavelength deviation is less than 10 nm. The fabrication error has a strong impact on the on-axis intensity distribution; when it occurs for the middle annulus, a more severe impact will be induced. The above findings provide theoretical guidance for applying multi-annular metasurfaces in the fields of super-resolution focusing, micro-nano fabrication, and nanoscopic imaging.

1. Introduction

The multi-annular metasurface, proposed in 2012 [1], is one type of planar nanostructured diffractive element. It is used to achieve far-field optical sub-diffraction and super-resolution without near-field evanescent waves [2–8]. The essence of the metasurface is due to the delicate interference of many diffracted beams [1], which essentially differs from lens-based optical focusing systems [9,10]. The multi-annular metasurface has been used to modulate super-resolving light spots [1,3,8,11] and ultra-thin optical needles [4,7,12]. The metasurface was originally designed based on the scalar angular spectrum theory and using the binary particle swarm algorithm [1]. It was then generalized to be the vectorial form based on the vectorial angular spectrum (VAS) theory [3]. Using the genetic algorithm and fast Hankel transform algorithm, various metasurfaces were designed [3,13,14]. Recently, the vectorial design theory has been rigorously tested by the three-dimensional (3D) finite-difference time-domain (FDTD) method [15].

However, general rules for selecting the material and thickness of the metallic film have not been reported so far, and the influence is not clear when the illumination wavelength deviates from the design wavelength. Besides, the fabrication error of the metasurface has not been studied. The above problems may restrict the practical application of metasurfaces in the fields of super-resolution focusing, micro-nano fabrication, and nanoscopic imaging. In this paper, the vectorial design theory and the FDTD method have been combined to explore the electromagnetic focusing properties of multi-annular nanostructured metasurfaces. Compared with other types of metasurfaces [16,17], the multi-annular metasurfaces are rotationally symmetric and easy-to-fabricated using current micromachining technology, e.g. focused ion beam (FIB).

2. Design theory

When a metasurface is normally illuminated by a polarized vector beam propagating along the positive direction of z axis, as shown in Fig. 1, the light field in any observation plane away from the mask surface can be determined according to the VAS theory if the electric field behind the metasurface is known [3,15].

For a linearly polarized beam (LPB, x-polarized), components of the electric field $\boldsymbol{E}$ for any point $P(r, \varphi, z)$ in the observation plane $(z > 0)$ can be described as [14,15]

* Corresponding author at: State Key Laboratory for Manufacturing System Engineering, Xi'an Jiaotong University, Xi'an 710049, China.
E-mail address: liu8483@xjtu.edu.cn (T. Liu).

http://dx.doi.org/10.1016/j.optcom.2016.04.021
0030-4018/

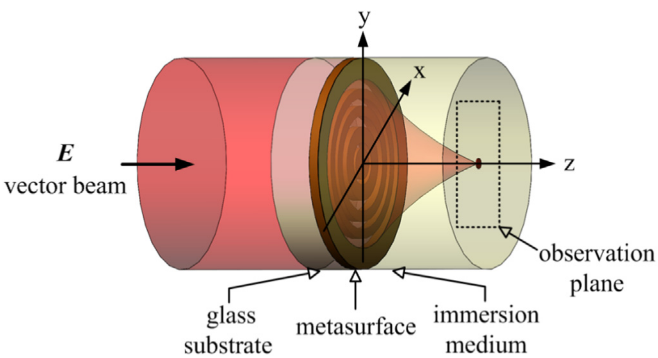

Fig. 1. Electromagnetic simulation model of a multi-annular metasurface.

$$\begin{cases} E_x(r,z) = \int_0^\infty A_0(l)\exp[j2\pi q(l)z]J_0(2\pi lr)2\pi l\mathrm{d}l \\ E_y(r,z) = 0 \\ E_z(r,\varphi,z) = -j\cos\varphi\int_0^\infty \frac{l}{q(l)}A_0(l)\exp[j2\pi q(l)z]J_1(2\pi lr)2\pi l\mathrm{d}l \end{cases} \quad (1)$$

where $q(l) = (1/\lambda^2 - l^2)^{1/2}$ and l is the transverse spatial frequency component. $\lambda = \lambda_0/n$ with λ_0 being the vacuum wavelength and n the refractive index of the immersion medium. J_0 and J_1 are the zeroth and first order Bessel functions of the first kind, respectively. For a uniform plane beam, $A_0(l)$ in Eq. (1) is expressed as

$$A_0(l) = \int_0^\infty t(r)J_0(2\pi lr)2\pi r\mathrm{d}r \quad (2)$$

where $t(x,y)$ represents the scalar transmission function for a metasurface, which is a basic assumption for all current design theories [1–4]. The total electric energy density (or light intensity) is calculated by $I(r,\varphi,z) = |\boldsymbol{E}(r,\varphi,z)|^2 = |E_x(r,z)|^2 + |E_z(r,\varphi,z)|^2$. For a circularly polarized beam (CPB) and a radially polarized beam, the integral formulae have been derived in [15] and [3], respectively.

3. Results and discussions

3.1. Test samples

Based on the vectorial design theory, $M_{1,4}$ and $M_{2,3}$ are designed with a CPB and a LPB, respectively, as summarized in Table 1. The specific optimization process is implemented using the genetic algorithm and fast Hankel transform algorithm [3,14]. The illumination wavelength is $\lambda_0 = 640$ nm. The diameters of $M_{1–4}$ are set to be 14 μm, which have 35 concentric rings with an equidistant annulus width of 200 nm. $M_{1,2}$ are placed in the oil immersion medium to increase the equivalent numerical aperture [3], which can sharpen the diffracted beam as well as the subwavelength focus. $M_{3,4}$ are optimized in air. The metasurfaces are coded with binary digits {0, 1} ('0' denoting an opaque annulus and '1' for a transparent annulus). The electromagnetic simulation model (Fig. 1) is physically solved by the 3D FDTD method in order to test the focusing properties of the metasurface [15]. The total-field scattered-field boundary and perfectly matched layer absorbing boundary are applied in the FDTD simulation. The metasurface is placed in air ($n = 1$) or oil ($n = 1.514$). The 3D simulation area is set to be x, y: −7.5–7.5 μm, and z: −2–8 μm. The mesh size for the metallic film is 15 nm × 15 nm × 5 nm (x, y, and z) and 15 nm × 15 nm × 20 nm for other regions.

Table 1
Optimized metasurfaces.

Item	Beam	Medium	$t_{1\sim35}$
M_1	CPB	oil	10101000110110010010010101100010100
M_2	LPB	oil	01100110100111101011100001010100101
M_3	LPB	air	00100110101110101011111111110001011
M_4	CPB	air	10000100110110110011011110011001101

3.2. Material property

To study the material property of the metasurface, three metallic film materials, Ag, Al, and Au, are compared with the thickness ranging from 25 nm to 200 nm with an increment of 25 nm. The schematic diagram of M_1 is shown in Fig. 2(a). As shown in Fig. 2(b), the main focus calculated by the VAS theory is located at $z_p = 2.88$ μm, where z_p is the focal length. However, z_p calculated by FDTD is slightly decreasing with the increase of the thickness for the three metal films. For the Al film, the focal length is always shorter than 2.88 μm. For the Au film, the focal length is no shorter than that obtained using the Ag and Al films except for the 20 nm and 200 nm thickness.

The full width at half maximum (FWHM) is used to characterize the size of the main focus. For the Al film, $FWHM_z$ (the axial size) and $FWHM_x$ (the transverse size) monotonically increase with the increase of thickness, as shown in Fig. 2(c); when the film thickness is larger than 75 nm, $FWHM_z$ and $FWHM_x$ obviously widen. For these three films, the minimum $FWHM_x$ of the main focus is as small as 241.6 nm ($0.38\lambda_0$) using the 20 nm-thick Au film. The peak intensity of the main focus also depends on the film material and thickness, as shown in Fig. 2(d). For the Al film, the peak intensity gradually decreases with the increase of thickness; however, for the Ag and Au films, the peak intensity first increases and then decreases. So it can be concluded that an obvious focal shift is produced, and in order to obtain the optimal focusing property, the thickness for the Ag, Al and Au films is suggested to be within the range of 50–100 nm for the illumination wavelength of 640 nm.

It should be indicated that, the opaque annuli of a metasurface should be practically realized by coating some metallic films on the glass substrate, and the metallic film needs to be sufficiently thick to attenuate the incident light. This accounts for the unavoidable difference between the theoretical result (VAS) and the FDTD-simulated result. It is also known that different metal materials have distinct electromagnetic properties. These are characterized by the permittivity (ε) and magnetic permeability (μ), which will have a significant impact on the light propagating property. These inherent differences have been physically modeled in the FDTD simulation. Different thicknesses and electromagnetic properties are set for different metal materials, so the focusing properties are different. However, currently it is difficult to more deeply clarify the mechanism, which requires further researches.

3.3. Dispersion property

To study the dispersion property of multi-annular metasurfaces, $M_{2,3}$ are particularly tested using the Au film with a 100 nm-thickness of 100 nm by using the LPB in the oil medium and the air medium, respectively. The on-axis intensity distributions calculated by FDTD are plotted in Fig. 3. The results for M_2 are shown in Fig. 3(a) and (b). For M_3, the results are shown in Fig. 3(c) and (d). All the curves in Fig. 3 have been normalized by respective peak intensities. The black dashed lines correspond to the results obtained with the designed illumination wavelength (640 nm).

For M_2, when the wavelength deviation is within 10 nm, the